Crosstalk between chloroplast protein import and the SUMO system revealed through genetic and molecular investigation

Samuel Watson[1†], Na Li[1], Feijie Wu[2‡], Qihua Ling[1,2‡], R. Paul Jarvis[1,2*]

[1]Department of Plant Sciences, University of Oxford, Oxford OX1 3RB, UK.

[2]Department of Biology, University of Leicester, Leicester LE1 7RH, UK.

[†]Present address: Cambridge Institute for Therapeutic Immunology and Infectious Disease, Jeffrey Cheah Biomedical Centre, University of Cambridge, Cambridge CB2 0AW, UK.

[‡]Present address: National Key Laboratory of Plant Molecular Genetics, CAS Centre for Excellence in Molecular Plant Sciences, Institute of Plant Physiology and Ecology, Shanghai Institutes for Biological Sciences, Chinese Academy of Sciences, Shanghai, China.

*For correspondence: paul.jarvis@plants.ox.ac.uk

Abstract

The chloroplast proteome contains thousands of different proteins that are encoded by the nuclear genome. These proteins are imported into the chloroplast via the action of the TOC translocase and associated downstream systems. Our recent work has revealed that the stability of the TOC complex is dynamically regulated via the ubiquitin-dependent chloroplast-associated protein degradation (CHLORAD) pathway. Here, we demonstrate that the stability of the TOC complex is also regulated by the SUMO system. *Arabidopsis* mutants representing almost the entire SUMO conjugation pathway can partially suppress the phenotype of *ppi1*, a pale yellow mutant lacking the Toc33 protein. This suppression is linked to increased stability of TOC proteins and enhanced chloroplast development. In addition, we demonstrate using molecular and biochemical experiments that the SUMO system directly targets TOC proteins. Thus, we have identified a regulatory link between the SUMO system and chloroplast protein import.

Introduction

The chloroplast is a membrane-bound organelle that houses photosynthesis in all green plants (Jarvis and Lopez-Juez, 2013). Chloroplasts have an unusual evolutionary history – they are the integrated descendants of a free-living cyanobacterial ancestor that entered the eukaryotic lineage via endosymbiosis. Although chloroplasts retain small genomes, almost all of the proteins required for chloroplast development and function are now encoded by the central, nuclear genome (Jarvis, 2008). These proteins must be imported into the organelle after synthesis in the cytosol, and this import is mediated by the coordinate action of the TOC and TIC complexes (the translocons at the outer and inner envelope membranes of chloroplasts) (Jarvis, 2008).

The TOC complex contains three major components: the Omp85 (outer membrane protein, 85 kD)-related protein, Toc75, which serves as a membrane channel (Schnell et al., 1994; Tranel et al., 1995), and two GTPase-domain receptor proteins, Toc33 and Toc159 (Hirsch et al., 1994; Kessler et al., 1994; Perry and Keegstra, 1994; Jarvis et al., 1998; Jarvis, 2008). Toc33 and Toc159 project out into the cytosol and bind incoming preproteins.

The key components of the TOC complex were identified more than two decades ago (Hirsch et al., 1994; Kessler et al., 1994; Schnell et al., 1994; Tranel et al., 1995; Jarvis, 2008). However, the regulation of the activity and stability of the complex was, until recently, poorly understood. Major insights came from a forward genetic screen for suppressors of the pale yellow Toc33 mutant, *ppi1* (Ling et al., 2012). As a result of this screen, a novel RING-type E3 ubiquitin ligase, SP1 (SUPPRESSOR OF PPI1 LOCUS 1), was identified. A series of *sp1* mutants were shown to partially suppress the phenotypic defects of *ppi1* with respect to chlorosis, chloroplast development, and chloroplast protein import. In addition, SP1 function was shown to promote plastid interconversion events (for example, the development of the chloroplast from its precursor organelle, the etioplast). Later work demonstrated that SP1 function is also important for abiotic stress tolerance, by enabling optimisation of the organellar proteome via protein import regulation (Ling and Jarvis, 2015). Thus, through SP1, the ubiquitin-proteasome system promotes TOC complex degradation and reconfiguration in response to developmental and/or environmental stimuli.

Ubiquitinated TOC proteins are extracted from the chloroplast outer envelope membrane and degraded in the cytosol. Recent work identified two proteins that physically associate with SP1 and promote the membrane extraction of TOC proteins (Ling et al., 2019). These are SP2, an Omp85-type β-barrel channel protein that was identified in the same genetic screen as SP1, and Cdc48, a well-characterised cytosolic AAA+ chaperone ATPase that provides the motive force for the extraction of proteins from the chloroplast outer envelope. The three proteins – SP1, SP2 and Cdc48 – together define a new pathway for the ubiquitination, membrane extraction, and degradation of chloroplast outer envelope proteins, which has been named chloroplast-associated protein degradation, or CHLORAD. In addition to CHLORAD, there exist cytosolic ubiquitin-dependent systems that also contribute to chloroplast biogenesis, by regulating the levels of unimported preproteins (Lee et al., 2009; Grimmer et al., 2020), and by controlling the stability of the Toc159 receptor prior to its integration into the outer envelope membrane (Shanmugabalaji et al., 2018).

The discovery of SP1 and the CHLORAD pathway demonstrated that the TOC complex is not static but, instead, can be rapidly ubiquitinated and degraded in response to developmental and environmental stimuli. To complement this work, we decided to explore whether the TOC complex is also regulated by the SUMO system. This work was motivated by the results of a high-throughput screen for SUMO substrates in *Arabidopsis* (Elrouby and Coupland, 2010). This screen suggested that Toc159, a key component of the TOC complex, is a SUMO substrate. SUMOylation is intricately

involved in plant development and stress adaptation, and so we were interested to determine whether the TOC complex is targeted by the SUMO target, and whether this SUMOylation is functionally important. As crosstalk between the SUMO system and the ubiquitin-proteasome system is common, we reasoned that answering these questions might provide insights into the regulation of SP1 and the CHLORAD pathway.

To explore the relationship between chloroplast protein import and the SUMO system, we carried out a comprehensive series of genetic, molecular and biochemical experiments. Mutants representing most components of the *Arabidopsis* SUMO pathway were found to partially suppress the phenotype of the chlorotic Toc33 null mutant, *ppi1*, with respect to leaf chlorophyll accumulation, chloroplast development, and TOC protein abundance. Conversely, overexpression of either *SUMO1* or *SUMO3* enhanced the severity of the *ppi1* phenotype. Moreover, the E2 SUMO conjugating enzyme, SCE1, was found to physically interact with the TOC complex in bimolecular fluorescence complementation experiments; and TOC proteins were seen to physically associate with SUMO proteins in immunoprecipitation assays. In combination, our data conclusively demonstrate significant crosstalk between the SUMO system and chloroplast protein import, and emphasise the complexity of the regulation of the TOC translocase.

Results

The E2 SUMO conjugating enzyme mutant, *sce1-4*, and the E3 SUMO ligase mutant, *siz1-4*, partially suppress the Toc33 mutant, *ppi1*

Two key components of the CHLORAD pathway, SP1 and SP2, were identified in a forward genetic screen for suppressors of the *Arabidopsis* Toc33 null mutant, *ppi1* (Ling et al., 2012; Ling et al., 2019). Both *sp1* and *sp2* mutants can partially suppress *ppi1* with respect to chlorophyll accumulation, chloroplast development, and TOC protein abundance. Thus, in an effort to determine whether the TOC complex is targeted by the SUMO system, we obtained several *Arabidopsis* SUMO system mutants and crossed them with *ppi1*, and then carefully examined the phenotypes of the resulting double mutants.

First, we analysed *sce1-4*, an E2 SUMO conjugating enzyme mutant. SCE1 is the only known E2 SUMO conjugating enzyme in *Arabidopsis* and it is essential (Saracco et al., 2007). The *sce1-4* mutant shows a moderate reduction in the expression of SCE1 but displays no obvious phenotypic defects under steady-state conditions (Saracco et al., 2007). The *ppi1 sce1-4* double mutant was phenotypically characterised, and, intriguingly, it appeared greener than the *ppi1* single mutant when grown on soil (Figure 1A). This was linked to a moderate increase in leaf chlorophyll concentration (Figure 1B). Next, we asked whether the phenotypic suppression observed in *ppi1 sce1-4* was linked to changes in the development of chloroplasts. The chloroplasts of *ppi1 sce1-4* were visualised via transmission electron microscopy. Interestingly, the chloroplasts of the *ppi1 sce1-4* double mutant appeared larger and better developed than those of the *ppi1* control (Figure 1C). The transmission electron micrographs were quantitatively analysed, and the *ppi1 sce1-4* chloroplasts were indeed found to be significantly larger than those of *ppi1* (Figure 1D), with larger, more interconnected thylakoidal granal stacks (Figures 1E and 1F).

SUMO conjugation is usually dependent on the action of E3 SUMO ligases. In *Arabidopsis*, the best characterised E3 SUMO ligase is SIZ1 (Kurepa et al., 2003; Miura et al., 2005; Saracco et al., 2007). SIZ1 is not essential, but null mutants display severely dwarfed phenotypes. In order to include SIZ1 in our genetic analysis, it was necessary to identify a new mutant that had a less severe phenotype than the null mutants. To this end, we obtained two new T-DNA insertion alleles, and named them

siz1-4 and *siz1-5.* One of the mutants, *siz1-4*, showed a milder phenotype than published mutants – it showed only moderate growth retardation when grown to maturity. The two *siz1* mutants were crossed with *ppi1* and the resulting double mutants were phenotypically characterised. Both the *ppi1 siz1-4* and the *ppi1 siz1-5* double mutants appeared greener than the *ppi1* control when grown on soil (Figure 1G). In addition, the *ppi1 siz1-4* double mutant showed a dramatic increase in leaf chlorophyll concentration relative to *ppi1* (Figure 1H). Next, we asked if the phenotypic suppression observed in *ppi1 siz1-4* was linked to changes in the abundance of TOC proteins. Protein samples were taken from the mature leaves of the double mutant (and relevant control plants) and resolved via immunoblotting. Intriguingly, the *ppi1 siz1-4* double mutant displayed a robust increase in the abundance of Toc159 and Toc75, two core components of the TOC complex (Figure 1I). In contrast, the abundance of Tic110 and Tic40, two TIC complex proteins which were included here as controls, was unaffected.

The suppression effects mediated by the SUMO system mutants are specific

A large number of proteins are subject to SUMOylation in *Arabidopsis*; however, the SUMO system is encoded by only a small number of genes. Thus, SUMO system mutants have highly pleiotropic molecular and physiological phenotypes. We therefore asked whether the partial suppression of *ppi1* by SUMO system mutants was specific to the *ppi1* background. To address this question, we crossed *sce1-4* with two pale, TIC complex associated mutants – *tic40-4* and *hsp93-V-I*. These mutants are chlorotic due to defects in protein import across the chloroplast inner membrane and in this respect are highly similar to *ppi1* (Kovacheva et al., 2005). Significantly, the resulting double mutants, *tic40-4 sce1-4* and *hsp93-V-I sce1-4*, were indistinguishable from their respective single mutant controls (*tic40-4* and *hsp93-V-I*) (Figures 2A and 2C). Moreover, the double mutants did not display increases in leaf chlorophyll accumulation relative to the single mutant controls (Figures 2B and 2D). Therefore, we concluded that the suppression effects observed in *ppi1 sce1-4* were highly background-specific and were tightly associated with the TOC complex.

Next, we asked whether the *sce1-4* and *siz1-4* single mutants display an increase in chlorophyll concentration even in the wild-type background. However, neither mutant appeared greener than wild-type plants (Figures 2E and 2G) or displayed an increase in leaf chlorophyll concentration (Figures 2F and 2H). This was particularly noteworthy in the case of *siz1-4*, as the *ppi1 siz1-4* double mutant displayed near complete phenotypic suppression with respect to leaf chlorophyll concentration (Figure 1H). Thus, we concluded that the suppression effects mediated by both mutants, as shown in Figure 1, were synthetic phenotypes specific to the *ppi1* background.

BiFC analysis reveals that SCE1 physically interacts with TOC proteins

Our reverse genetic experiments revealed a genetic link between the E2 SUMO conjugating enzyme, SCE1, and protein import across the chloroplast outer membrane. To determine whether SCE1 directly interacts with the TOC complex, bimolecular fluorescence complementation (BiFC) experiments were performed in *Arabidopsis* protoplasts. To this end, the *SCE1* coding sequence was inserted into a vector that C-terminally appends the N-terminal half of YFP (nYFP). This construct was co-expressed with various other constructs encoding TOC proteins bearing the complementary, C-terminal moiety of the YFP protein (cYFP), appended C-terminally. In this system, protein-protein interactions are inferred via the detection of a YFP signal, caused by the nYFP and cYFP fragments coming together to reconstitute a functional YFP protein.

Strikingly, SCE1-nYFP was found to physically associate with all tested TOC proteins – Toc159-cYFP, Toc132-cYFP, Toc34-cYFP and Toc33-cYFP (Figure 3). Moreover, these interactions were

concentrated at the periphery of the chloroplasts, placing them in an appropriate subcellular context for the *in situ* regulation of the chloroplast protein import machinery. Conversely, SCE1-nYFP was not found to physically associate with the negative control protein ΔOEP7-cYFP. This protein comprises the transmembrane domain of plastid protein OEP7 fused to the cYFP fragment. The transmembrane domain of OEP7 is sufficient to efficiently target the full-length YFP protein to the chloroplast outer membrane (Lee et al., 2001); thus ΔOEP7-cYFP serves as a location-specific negative control.

Manipulating the expression of three SUMO isoforms alters the phenotypic severity of *ppi1*

The preceding genetic and molecular experiments revealed a clear link between the SUMO system and chloroplast protein import, implying that TOC proteins are SUMOylated. We therefore decided to carry out a series of experiments to assess for genetic interactions between genes encoding SUMO proteins and *ppi1*. There are three major SUMO isoforms in *Arabidopsis* – SUMO1, SUMO2, and SUMO3. The *SUMO1* and *SUMO2* genes are expressed at a relatively high level throughout the plant and are largely functionally redundant (Saracco et al., 2007; van den Burg et al., 2010). In addition, they are highly similar to each other in terms of amino acid sequence (Saracco et al., 2007). In contrast, at steady state, *SUMO3* is expressed at a relatively low level throughout the plant, while the SUMO3 amino acid sequence is significantly divergent with respect to the other two SUMO isoforms (van den Burg et al., 2010).

First, we analysed *SUMO1* and *SUMO2*. We obtained *sum1-1* and *sum2-1*, two previously characterised *Arabidopsis* null mutants (Saracco et al., 2007), and crossed them with *ppi1*. To account for the functional redundancy between these two genes, we also sought a *ppi1 sum1-1 sum2-1* triple mutant. However, as *SUMO1* and *SUMO2* are collectively essential, *ppi1 sum1-1 sum2-1* plants that were homozygous with respect to *ppi1* and *sum2-1*, but heterozygous with respect to the *sum1-1* mutation, were selected from a segregating population. The double and triple mutants were phenotypically characterised, and all three appeared larger and greener than the *ppi1* control plants (Figure 4A). Moreover, the double and triple mutants showed corresponding increases in leaf chlorophyll concentration, with the triple mutant showing a larger increase than the double mutants (Figure 4B). Therefore, we concluded that the *sum1-1* and *sum2-1* mutants can additively suppress the phenotype of *ppi1*.

To complement the above-described experiment, we generated transgenic plants overexpressing *SUMO1* in the *ppi1* background. The *SUMO1* coding sequence was cloned into a vector carrying a strong, constitutive promotor (cauliflower mosaic virus 35S) upstream of the cloning site. The resulting construct was stably introduced into the *ppi1* background via *Agrobacterium*-mediated transformation. Two lines carrying a single, homozygous transgene insert were identified and taken forward for analysis. The overexpression of *SUMO1* was confirmed in both lines via semi-quantitative RT-PCR (Figure 4 supplement, panel A). Significantly, both lines displayed an accentuation of the *ppi1* phenotype – the plants were significantly smaller and paler than the *ppi1* control plants (Figure 4C), and showed decreases in leaf chlorophyll concentration (Figure 4D).

Next, we turned our attention to *SUMO3*. We obtained *sum3-1*, a previously characterised null mutant (van den Burg et al., 2010), and crossed it with *ppi1*. The resulting double mutant was phenotypically characterised, and, interestingly, it did not appear obviously different from the *ppi1* control (Figure 4E). Correspondingly, it did not display any clear increase in leaf chlorophyll concentration relative to *ppi1* (Figure 4F). To complement this experiment, we generated transgenic plants overexpressing *SUMO3* in the *ppi1* background, using the approach described above, and a line carrying a single, homozygous insert was identified and taken forward for analysis. The

overexpression of *SUMO3* was confirmed via semi-quantitative RT-PCR (Figure 4 supplement, panel B). Interestingly, the transgenic plants showed a striking increase in the severity of the *ppi1* phenotype – the plants were severely dwarfed and paler than the *ppi1* control (Figure 4G), and displayed a significant decrease in leaf chlorophyll accumulation (Figure 4H). These findings are particularly noteworthy when considered alongside a previous report which explored the consequences of overexpressing *SUMO3* in wild-type plants (van den Burg et al., 2010). In that previous work, *SUMO3* overexpression was not found to alter the appearance of the transgenic plants, which implies a degree of specificity in the phenotypic accentuation observed here.

Biochemical analysis reveals SUMOylation of TOC proteins *in vivo*

The genetic and molecular experiments described thus far strongly suggested that TOC proteins are SUMOylated. However, to our knowledge, conclusive evidence that chloroplast-resident proteins are SUMOylated is currently lacking. Therefore, to investigate whether chloroplast proteins may be SUMOylated, we isolated chloroplasts from seedlings by cell fractionation, and analysed them by anti-SUMO immunoblotting. For this analysis, we employed a proven commercial antibody against SUMO1, which is one of the most abundant SUMO isoforms in *Arabidopsis* making it more tractable for analysis, and which furthermore is known to accumulate in response to heat and other stresses (Kurepa et al., 2003; van den Burg et al., 2010). With the goal of enhancing the detection of SUMOylated proteins in our samples, we subjected some of the seedlings to heat shock before chloroplast isolation and/or treatment with 10 mM N-ethylmaleimide (NEM) during chloroplast isolation; NEM is a potent inhibitor of SUMO-specific proteases (Hilgarth and Sarge, 2005). Importantly, we detected protein SUMOylation in the isolated chloroplast samples, and this SUMOylation was increased by NEM treatment (Figure 5 supplement 1).

Next, we sought to determine whether TOC proteins are SUMOylated. To test this idea directly, a number of biochemical experiments were performed. In the first of these, the *SCE1* coding sequence was cloned into a vector that appends a C-terminal YFP tag (Karimi et al., 2002). The resulting SCE1-YFP construct expressed well and showed the expected nucleocytoplasmic fluorescence pattern when transiently expressed in *Arabidopsis* protoplasts (Figure 5 supplement 2, panel A). Thus, larger numbers of protoplasts were transfected with the SCE1-YFP construct, or a YFP-HA negative control construct, and the transfected cells were solubilised and incubated with YFP-Trap magnetic beads. After incubation, the beads were magnetically separated from the lysate, then boiled in loading buffer to release bound proteins. The eluted proteins, along with total lysate and flow-through samples, were analysed by immunoblotting. The YFP-HA and SCE1-YFP fusion proteins both showed robust expression, and strong recovery in the IP fractions (Figure 5A). By analysing the samples using a range of other antibodies, the SCE1-YFP fusion protein was found to be associated with native Toc159 and Toc132 but not with the negative control proteins Tic110 or Tic40 (Figure 5A). Conversely, YFP-HA did not associate with any of the tested proteins.

In the second experiment, we cloned the *SUMO1*, *SUMO2*, and *SUMO3* coding sequences into a vector that appends an N-terminal YFP tag (Karimi et al., 2002), a modification which previous studies have shown to be tolerated (Ayaydin and Dasso, 2004). All three constructs expressed well and showed the expected nucleocytoplasmic fluorescence pattern when transiently expressed in protoplasts (Figure 5 supplement 2, panel B). The three constructs were expressed in parallel in protoplasts, as well as the YFP-HA negative control construct. As in the previous experiment, solubilised protoplasts were subjected to YFP-Trap immunoprecipitation, and protein samples were analysed by immunoblotting. Remarkably, all three YFP-SUMO proteins were found to physically associate with Toc159, although YFP-SUMO3 clearly bound Toc159 with the greatest affinity (Figure 5B). Moreover, inspection of an extended exposure of the anti-YFP blot revealed a number of higher

molecular weight bands that we interpret to be SUMO adducts and indicative of the functionality of the fusions (Figure 5 supplement 3). In contrast with the SUMO fusions, the YFP-HA negative control did not associate with Toc159; and none of the four SUMO fusion proteins physically associated with Tic40, a negative control protein (Figure 5B).

The immunoprecipitation experiment described above identified SUMO3 as having the highest affinity for Toc159. To extend our analysis of SUMO3 to include another TOC protein, and to provide more direct evidence for TOC protein SUMOylation, the experiment was repeated with modifications, as follows. Protoplasts were co-transfected with YFP-SUMO3 and Toc33-HA, or YFP-HA and Toc33-HA; in each case, the transient overexpression of Toc33 was done to aid detection of this component and its adducts. The construct pairs were co-expressed in protoplasts, and then the samples were subjected to YFP-Trap immunoprecipitation analysis, as described earlier. In accordance with the Toc159 result (Figure 5B), YFP-SUMO3, but not YFP-HA, was found to physically associate with Toc33-HA (Figure 5C). Moreover, bands of the exact expected molecular weight of Toc33-HA bearing one or two YFP-SUMO3 moieties (75 and 114 kDa) were also detected. These bands were accompanied by a high molecular weight smear at the top of the immunoblot, which is indicative of complex, multisite or chain SUMOylation.

Discussion

This work has revealed a genetic and molecular link between the SUMO system and chloroplast protein import. The genetic experiments demonstrated that SUMO system mutants can suppress the phenotype of the Toc33 mutant, *ppi1*, and the molecular and biochemical experiments indicated that TOC proteins associate with key SUMO system proteins and are SUMOylated. Visible suppression effects observed in the *ppi1* / SUMO system double mutants were linked to improvements in chloroplast development and enhanced accumulation of key TOC proteins. Importantly, each core TOC protein, including all of those analysed in this study, was predicted with high probability to have one or more SUMOylation sites (Table 1) (Zhao et al., 2014; Beauclair et al., 2015).

The *ppi1* suppression effects described here are remarkably similar to those mediated by the *sp1* and *sp2* mutants (Ling et al., 2012; Ling et al., 2019). Like *sp1* and *sp2*, SUMO system mutants can partially suppress *ppi1* with respect to chlorophyll concentration, TOC protein accumulation, and chloroplast development. This similarity suggests that SUMOylation may regulate the activity of the CHLORAD pathway. This is an attractive hypothesis, as both SUMOylation and the CHLORAD pathway are activated by various forms of environmental stress (Kurepa et al., 2003; Ling and Jarvis, 2015; Ling et al., 2019). One possibility is that SUMOylation of TOC proteins promotes their CHLORAD-mediated degradation. Certainly, the ability to carry out SUMOylation is negatively correlated with the stability of TOC proteins in the context of the developed plants studied here. However, it should be kept in mind that SUMOylation can both promote and antagonise the effects of ubiquitination, in different situations (Desterro et al., 1998; Ahner et al., 2013; Liebelt and Vertegaal, 2016); and so our results do not preclude the possibility that SUMOylation may have different consequences for chloroplast biogenesis in other contexts. The Toc159 receptor is regulated by SP1 when integrated into the outer envelope membrane (Ling et al., 2012; Ling et al., 2019), but by a different E3 ligase when it exists as a cytosolic precursor during the earliest stages of development before germination (Shanmugabalaji et al., 2018). Thus, regulation by SUMOylation might be similarly different in these two distinct developmental contexts.

The precise mechanisms underpinning the observed negative regulation of the TOC apparatus by SUMOylation are currently unknown. One possibility is that the SUMOylation of TOC proteins

promotes their association with SP1. SUMOylation can modify protein-protein interactions, and some RING-type E3 ubiquitin ligases specifically recognise SUMOylated substrates (Sriramachandran and Dohmen, 2014). However, these SUMO-targeted ubiquitin ligases (STUbLs) typically contain SUMO-interacting motifs (SIMs) which guide the ligases to SUMO proteins conjugated to their substrates, and these are not apparent in SP1 (data not shown) (Zhao et al., 2014). However, SP1 forms a complex with SP2 and very likely additional cofactors, and these could hypothetically provide a SUMO binding interface. Another possibility is that SUMOylation could be involved in the recruitment of Cdc48 from the cytosol. Two important Cdc48 cofactors are Ufd1 and Npl4, and the former contains a SUMO-interacting motif which can guide Cdc48 to SUMOylated proteins (Nie et al., 2012; Baek et al., 2013). Moreover, the SUMO-mediated recruitment of Cdc48 has important roles in the maintenance of genome stability in yeast (Bergink et al., 2013).

The biochemical experiments described herein indicate that, of the three SUMO isoforms tested, SUMO3 binds TOC proteins with the highest affinity. However, there is an apparent incongruence between the results of these experiments and the results of the genetic experiments. While the *sum1-1* and *sum2-1* mutants were found to additively suppress *ppi1*, the *sum3-1* mutant did not suppress *ppi1*. At face value, this seems puzzling; however, it can be explained by the relative abundance of the three SUMO proteins *in planta*. SUMO1 and SUMO2 are highly abundant relative to SUMO3, which is, at steady state, very weakly abundant (van den Burg et al., 2010). The immunoprecipitation data shown in Figure 5B indicated that SUMO1 and SUMO2 can weakly interact with Toc159, and so it is likely that these two isoforms can compensate for the loss of SUMO3 in the *sum3-1* mutant. Although SUMO3 associates with TOC proteins with the highest affinity, the higher abundance of the other two SUMO proteins may facilitate such compensation.

It is now well established that the regulation of chloroplast protein import has critical roles in plant development and stress acclimation (Sowden et al., 2018; Watson et al., 2018). Here, we demonstrate regulatory crosstalk between the SUMO system and chloroplast protein import, and present results which are consistent with a model in which SUMOylation modulates the activity or effects of the CHLORAD pathway. The precise nature of the links between these two critically important control systems will be the subject of future investigation.

Materials and methods

Plant material and growth conditions

All *Arabidopsis thaliana* plants used in this work were of the Columbia-0 (Col-0) ecotype. The mutants used in almost all of the analyses (*ppi1*, *sce1-4*, *sum1-1*, *sum2-1*, *sum3-1*, *hsp93-V-I*, *tic40-4*) have been described previously (Jarvis et al., 1998; Kovacheva et al., 2005; Saracco et al., 2007; van den Burg et al., 2010). The *siz1-4* (SAIL_805_A10) and *siz1-5* (SALK_111280) mutants were obtained from the Salk Institute Genomic Analysis Laboratory (SIGnAL) (Alonso et al., 2003), via the Nottingham *Arabidopsis* Stock Centre (NASC). Each line was verified via PCR genotyping (see Table 2 for primer sequences) and phenotypic analysis (including the double and triple mutants).

In most experiments, plants were grown on soil (80% (v/v) compost (Levington M2), 20% (v/v) vermiculite (Sinclair Pro, medium particle size)). However, where plants were grown for selection of transformants or for chloroplast isolation, seeds were surface sterilised and sown on petri plates containing Murashige-Skoog (MS) agar medium. The plates were stored at 4°C for 48 hours before being transferred to a growth chamber. Both soil-grown and plate-grown plants were kept in a growth chamber (Percival Scientific) under long-day conditions (16 hours light, 8 hours dark). The

light intensity was approximately 120 µE m^{-2} s^{-1}, the temperature was held constant at 20°C, and the humidity was held constant at approximately 70% (relative humidity).

Chlorophyll measurements

Chlorophyll measurements were taken from mature rosette leaves in each instance. A handheld Konica-Minolta SPAD-502 meter was used to take each measurement, and the raw values were converted into chlorophyll concentration values (nmol/mg tissue) via published calibration equations (Ling et al., 2011).

Chloroplast isolation and protein extraction

Chloroplasts were isolated from 14-day-old, plate-grown seedlings as described previously (Flores-Pérez and Jarvis, 2017). Some of the seedlings were heat-shocked immediately prior to chloroplast isolation. To do this, the plates containing the seedlings were wrapped in clingfilm and placed into a water bath (42°C for 30 seconds). Protein samples were prepared from the isolated chloroplasts by extraction using SDS-PAGE sample buffer, as well as from whole 14-day-old seedlings as previously described (Kovacheva et al., 2005). In some cases, the samples were treated with 10 mM N-ethylmaleimide (Hilgarth and Sarge, 2005); this was added directly to the protein extraction buffer (whole seedling samples), or to the chloroplast isolation buffer following polytron homogenization and all subsequent buffers (chloroplast samples).

Plasmid constructs

The constructs used in the BiFC experiments were generated as follows. The coding sequences of *SCE1*, *SIZ1*, *TOC159*, *TOC132*, *TOC34*, *TOC33* and *SFR2* were PCR amplified from wild-type cDNA (see Table 2 for primer sequences). In the case of *ΔOEP7*, the first 105 base pairs of the *OEP7* coding sequence were amplified; this encodes a truncated sequence which is sufficient to efficiently target the full-length YFP protein to the chloroplast outer envelope membrane (Lee et al., 2001). The inserts were cloned into one of the following complementary vectors: pSAT4(A)-nEYFP-N1 (*SCE1*), pSAT4-cEYFP-C1-B (*TOC159*, *TOC132*, *TOC34*, *TOC33*), or pSAT4(A)-cEYFP-N1 (*ΔOEP7*, *SFR2*), which were described previously (Tzfira et al., 2005; Citovsky et al., 2006).

The constructs used in the immunoprecipitation experiments were generated as follows. The coding sequences of *SCE1*, *SUMO1*, *SUMO2* and *SUMO3* were PCR amplified from wild-type cDNA using primers bearing 5' attB1 and attB2 adaptor sequences (see Table 2 for primer sequences). The amplicons were then cloned into pDONR221 (Invitrogen), a Gateway entry vector. The inserts from the resulting entry clones were then transferred to one of two destination vectors: p2GWY7 (*SCE1*) or p2YGW7 (*SUMO1*, *SUMO2*, *SUMO3*); the former appends a C-terminal YFP tag to its insert, and the latter appends an N-terminal YFP tag to its insert (Karimi et al., 2002; Karimi et al., 2005). The Toc33-HA and YFP-HA constructs have been described previously (Ling et al., 2019).

The constructs used to generate transgenic plants were generated as follows. The coding sequences of *SUMO1* and *SUMO3* were PCR amplified from wild-type cDNA using primers bearing 5' attB1 and attB2 adaptor sequences (see Table 2 for primer sequences). The inserts were then cloned into pDONR201 (Invitrogen), a Gateway entry vector. The inserts from the resulting entry clones were then transferred to the pH2GW7 binary destination vector (Karimi et al., 2002; Karimi et al., 2005).

Transient expression assays

Protoplasts were isolated from mature rosette leaves of wild-type *Arabidopsis* plants and transfected in accordance with an established method (Wu et al., 2009; Ling et al., 2012). In the BiFC

experiments, 100 µL protoplast suspension (containing approximately 10^5 protoplasts) was transfected with 5 µg plasmid DNA; and in the immunoprecipitation experiments, 600 µL protoplast suspension (containing approximately 6×10^5 protoplasts) was transfected with 30 µg plasmid DNA. In both cases, the samples were analysed after 15-18 hours.

Stable plant transformation

Transgenic lines carrying the *SUMO1-OX* or *SUMO3-OX* constructs were generated via *Agrobacterium*-mediated floral dip transformation (Clough and Bent, 1998). Transformed plants (T_1 generation) were selected on MS medium containing phosphinothricin. Multiple T_2 families were analysed in each case, and lines bearing a single T-DNA insertion were taken forward for further analysis. Transgene expression was analysed by semi-quantitative RT-PCR as described previously (Kasmati et al., 2011) (see Table 2 for primer sequences).

Transmission electron microscopy

Transmission electron micrographs were recorded using mature rosette leaves as previously described (Huang et al., 2011). Images were taken from three biological replicates (different leaves from different individual plants), and at least 10 images were taken per replicate. The images were analysed using ImageJ (Schneider et al., 2012). The freehand tool was used to measure the plan area of the chloroplasts. For this, between 9 and 28 chloroplasts were analysed for each biological replicate (i.e., for each plant), and then an average value for each replicate was calculated and used for statistical comparisons. The analysis of chloroplast ultrastructure was performed as in previous work (Huang et al., 2011). For this, between 3 and 8 chloroplasts were analysed per biological replicate, and the data were processed as above.

BiFC experiments

The BiFC experiments were carried out as described previously (Ling et al., 2019). Protoplasts were co-transfected with two constructs encoding fusion proteins bearing complementary fragments of the YFP protein (nYFP and cYFP) (Citovsky et al., 2006). After transfection and overnight incubation, the protoplasts were imaged using a Zeiss LSM 510 META laser-scanning confocal micro-scope (Carl Zeiss) and the presence and distribution, or absence, of a YFP signal was recorded.

Immunoblotting and immunoprecipitation

Protein extraction and immunoblotting were performed as described in previously (Kovacheva et al., 2005). Total protein samples extracted from 30-50 mg leaf tissue were typically analysed. To detect proteins, we used an anti-SUMO1 antibody (Ab5316, Abcam), an anti-Toc75-III-3 antibody (Kasmati et al., 2011), an anti-Toc159 antibody (Bauer et al., 2000), an anti-Tic110 antibody (Inaba et al., 2005), an anti-Tic40 antibody (Kasmati et al., 2011), and an anti-green fluorescent protein antibody (Sigma). In most cases, the secondary antibody used was anti-rabbit immunoglobulin G (IgG) conjugated with horseradish peroxidase (Santa Cruz Biotechnology); and protein bands were visualised via chemiluminescence using an ECL Plus Western blotting detection kit (GE Healthcare) and an LAS-4000 imager (Fujifilm). However, in the case of Figure 5 supplement 1, the secondary antibody was anti-rabbit IgG conjugated with alkaline phosphatase (Sigma), and the membrane was incubated with BCIP/NBT chromogenic substrate (Sigma).

The immunoprecipitation (IP) experiments were also carried out as described previously (Ling et al., 2019). Constructs encoding YFP-conjugated fusion proteins (YFP-HA, SCE1-YFP, YFP-SUMO1, YFP-SUMO2, YFP-SUMO3) were transiently expressed in protoplasts. In some cases, the constructs were co-expressed with a construct encoding Toc33-HA. The protoplasts were solubilised using IP buffer

containing 1% Triton X-100, and the resulting lysates were incubated with GFP-Trap beads (Chromotek). After four washes in IP buffer, the protein samples were eluted by boiling in SDS-PAGE loading buffer, and then analysed by immunoblotting.

Statistical analysis

The data from each experiment were analysed in R. In most cases, two-tailed T-tests were performed. However, in one case, a one-way ANOVA was performed in conjunction with a Tukey HSD test (as indicated in the figure legend). Asterisks in the figures indicate the level of significance, as follows: *, $p<0.05$; **, $p<0.01$; ***, $p<0.001$; ****, $p<0.0001$; *****, $p<0.00001$.

SUMO site prediction

The amino acid sequences of Toc159, Toc132, Toc120, Toc90, Toc75, Toc33 and Toc34 were retrieved from The *Arabidopsis* Information Resource (TAIR) website (Berardini et al., 2015). The GPS-SUMO algorithm was applied to all seven sequences (http://sumosp.biocuckoo.org/online.php) (Zhao et al., 2014). The 'high stringency' setting was applied. The *p*-values were generated by the GPS-SUMO algorithm, and hits that were accompanied by *p*-values exceeding $p=0.05$ were manually removed. The JASSA algorithm was also applied to all seven amino acid sequences (http://www.jassa.fr/index.php) (Beauclair et al., 2015). In this case, the 'high cut-off' setting was applied. The GPS-SUMO and JASSA algorithms use fundamentally different methodologies (Chang et al., 2018).

References and notes

Ahner, A., Gong, X., and Frizzell, R.A. (2013). Cystic fibrosis transmembrane conductance regulator degradation: cross-talk between the ubiquitylation and SUMOylation pathways. FEBS Journal **280,** 4430-4438.

Alonso, J.M., Stepanova, A.N., Leisse, T.J., Kim, C.J., Chen, H., Shinn, P., Stevenson, D.K., Zimmerman, J., Barajas, P., Cheuk, R., Gadrinab, C., Heller, C., Jeske, A., Koesema, E., Meyers, C.C., Parker, H., Prednis, L., Ansari, Y., Choy, N., Deen, H., Geralt, M., Hazari, N., Hom, E., Karnes, M., Mulholland, C., Ndubaku, R., Schmidt, I., Guzman, P., Aguilar-Henonin, L., Schmid, M., Weigel, D., Carter, D.E., Marchand, T., Risseeuw, E., Brogden, D., Zeko, A., Crosby, W.L., Berry, C.C., and Ecker, J.R. (2003). Genome-wide insertional mutagenesis of *Arabidopsis thaliana*. Science **301,** 653-657.

Ayaydin, F., and Dasso, M. (2004). Distinct in vivo dynamics of vertebrate SUMO paralogues. Molecular Biology of the Cell **15,** 5208-5218.

Baek, G.H., Cheng, H., Choe, V., Bao, X., Shao, J., Luo, S., and Rao, H. (2013). Cdc48: a swiss army knife of cell biology. Journal of Amino Acids **2013,** 183421.

Bauer, J., Chen, K., Hiltbunner, A., Wehrli, E., Eugster, M., Schnell, D., and Kessler, F. (2000). The major protein import receptor of plastids is essential for chloroplast biogenesis. Nature **403,** 203-207.

Beauclair, G., Bridier-Nahmias, A., Zagury, J.F., Saib, A., and Zamborlini, A. (2015). JASSA: a comprehensive tool for prediction of SUMOylation sites and SIMs. Bioinformatics **31,** 3483-3491.

Berardini, T.Z., Reiser, L., Li, D., Mezheritsky, Y., Muller, R., Strait, E., and Huala, E. (2015). The Arabidopsis information resource: Making and mining the "gold standard" annotated reference plant genome. Genesis **53,** 474-485.

Bergink, S., Ammon, T., Kern, M., Schermelleh, L., Leonhardt, H., and Jentsch, S. (2013). Role of Cdc48/p97 as a SUMO-targeted segregase curbing Rad51-Rad52 interaction. Nature Cell Biology **15,** 526-532.

Chang, C.C., Tung, C.H., Chen, C.W., Tu, C.H., and Chu, Y.W. (2018). SUMOgo: Prediction of sumoylation sites on lysines by motif screening models and the effects of various post-translational modifications. Scientific Reports **8,** 15512.

Citovsky, V., Lee, L.Y., Vyas, S., Glick, E., Chen, M.H., Vainstein, A., Gafni, Y., Gelvin, S.B., and Tzfira, T. (2006). Subcellular localization of interacting proteins by bimolecular fluorescence complementation *in planta*. Journal of Molecular Biology **362,** 1120-1131.

Clough, S.J., and Bent, A.F. (1998). Floral dip: a simplified method for *Agrobacterium*-mediated transformation of *Arabidopsis thaliana*. Plant Journal **16,** 735-743.

Desterro, J.M., Rodriguez, M.S., and Hay, R.T. (1998). SUMO-1 modification of IkappaBalpha inhibits NF-kappaB activation. Molecular Cell **2,** 233-239.

Elrouby, N., and Coupland, G. (2010). Proteome-wide screens for small ubiquitin-like modifier (SUMO) substrates identify Arabidopsis proteins implicated in diverse biological processes. Proceedings of the National Academy of Sciences of the United States of America **107,** 17415-17420.

Flores-Pérez, Ú., and Jarvis, P. (2017). Isolation and suborganellar fractionation of Arabidopsis chloroplasts. Methods in Molecular Biology **1511,** 45-60.

Grimmer, J., Helm, S., Dobritzsch, D., Hause, G., Shema, G., Zahedi, R.P., and Baginsky, S. (2020). Mild proteasomal stress improves photosynthetic performance in Arabidopsis chloroplasts. Nature Communications **11,** 1662.

Hilgarth, R.S., and Sarge, K.D. (2005). Detection of sumoylated proteins. Methods in Molecular Biology **301,** 329-338.

Hirsch, S., Muckel, E., Heemeyer, F., von Heijne, G., and Soll, J. (1994). A receptor component of the chloroplast protein translocation machinery. Science **266,** 1989-1992.

Huang, W.H., Ling, Q.H., Bedard, J., Lilley, K., and Jarvis, P. (2011). In vivo analyses of the roles of essential Omp85-related proteins in the chloroplast outer envelope membrane. Plant Physiology **157,** 147-159.

Inaba, T., Alvarez-Huerta, M., Li, M., Bauer, J., Ewers, C., Kessler, F., and Schnell, D.J. (2005). Arabidopsis Tic110 is essential for the assembly and function of the protein import machinery of plastids. Plant Cell **17,** 1482-1496.

Jarvis, P. (2008). Targeting of nucleus-encoded proteins to chloroplasts in plants. New Phytologist **179,** 257-285.

Jarvis, P., and Lopez-Juez, E. (2013). Biogenesis and homeostasis of chloroplasts and other plastids. Nature Reviews Molecular Cell Biology **14,** 787-802.

Jarvis, P., Chen, L.J., Li, H.M., Pete, C.A., Fankhauser, C., and Chory, J. (1998). An *Arabidopsis* mutant defective in the plastid general protein import apparatus. Science **282,** 100-103.

Karimi, M., Inze, D., and Depicker, A. (2002). GATEWAY vectors for *Agrobacterium*-mediated plant transformation. Trends in Plant Science **7,** 193-195.

Karimi, M., De Meyer, B., and Hilson, P. (2005). Modular cloning in plant cells. Trends Plant Science **10,** 103-105.

Kasmati, A.R., Töpel, M., Patel, R., Murtaza, G., and Jarvis, P. (2011). Molecular and genetic analyses of Tic20 homologues in *Arabidopsis thaliana* chloroplasts. Plant Journal **66,** 877-889.

Kessler, F., Blobel, G., Patel, H.A., and Schnell, D.J. (1994). Identification of two GTP-binding proteins in the chloroplast protein import machinery. Science **266,** 1035-1039.

Kovacheva, S., Bedard, J., Patel, R., Dudley, P., Twell, D., Rios, G., Koncz, C., and Jarvis, P. (2005). *In vivo* studies on the roles of Tic110, Tic40 and Hsp93 during chloroplast protein import. Plant Journal **41,** 412-428.

Kurepa, J., Walker, J.M., Smalle, J., Gosink, M.M., Davis, S.J., Durham, T.L., Sung, D.Y., and Vierstra, R.D. (2003). The small ubiquitin-like modifier (SUMO) protein modification system in Arabidopsis. Accumulation of SUMO1 and -2 conjugates is increased by stress. Journal of Biological Chemistry **278,** 6862-6872.

Lee, S., Lee, D.W., Lee, Y., Mayer, U., Stierhof, Y.D., Jurgens, G., and Hwang, I. (2009). Heat shock protein cognate 70-4 and an E3 ubiquitin ligase, CHIP, mediate plastid-destined precursor degradation through the ubiquitin-26S proteasome system in *Arabidopsis*. Plant Cell **21,** 3984-4001.

Lee, Y.J., Kim, D.H., Kim, Y.W., and Hwang, I. (2001). Identification of a signal that distinguishes between the chloroplast outer envelope membrane and the endomembrane system in vivo. Plant Cell **13,** 2175-2190.

Liebelt, F., and Vertegaal, A.C. (2016). Ubiquitin-dependent and independent roles of SUMO in proteostasis. American Journal of Physiology Cell Physiology **311,** C284-C296.

Ling, Q., and Jarvis, P. (2015). Regulation of chloroplast protein import by the ubiquitin E3 ligase SP1 is important for stress tolerance in plants. Current Biology **25,** 2527-2534.

Ling, Q., Huang, W., and Jarvis, P. (2011). Use of a SPAD-502 meter to measure leaf chlorophyll concentration in Arabidopsis thaliana. Photosynthesis Research **107,** 209-214.

Ling, Q., Huang, W., Baldwin, A., and Jarvis, P. (2012). Chloroplast biogenesis is regulated by direct action of the ubiquitin-proteasome system. Science **338,** 655-659.

Ling, Q., Broad, W., Trösch, R., Töpel, M., Demiral Sert, T., Lymperopoulos, P., Baldwin, A., and Jarvis, R.P. (2019). Ubiquitin-dependent chloroplast-associated protein degradation in plants. Science **363**.

Miura, K., Rus, A., Sharkhuu, A., Yokoi, S., Karthikeyan, A.S., Raghothama, K.G., Back, D., Koo, Y.D., Jin, J.B., Bressan, R.A., Yun, D.J., and Hasegawa, P.M. (2005). The Arabidopsis SUMO E3 ligase SIZ1 controls phosphate deficiency responses Proceedings of the National Academy of Sciences of the United States of America **102,** 9734-9734.

Nie, M., Aslanian, A., Prudden, J., Heideker, J., Vashisht, A.A., Wohlschlegel, J.A., Yates, J.R., and Boddy, M.N. (2012). Dual recruitment of Cdc48 (p97)-Ufd1-Npl4 ubiquitin-selective segregase by small ubiquitin-like modifier protein (SUMO) and ubiquitin in SUMO-targeted ubiquitin ligase-mediated genome stability functions. Journal of Biological Chemistry **287,** 29610-29619.

Perry, S.E., and Keegstra, K. (1994). Envelope membrane proteins that interact with chloroplastic precursor proteins. Plant Cell **6,** 93-105.

Saracco, S.A., Miller, M.J., Kurepa, J., and Vierstra, R.D. (2007). Genetic analysis of SUMOylation in Arabidopsis: conjugation of SUMO1 and SUMO2 to nuclear proteins is essential. Plant Physiology **145,** 119-134.

Schneider, C.A., Rasband, W.S., and Eliceiri, K.W. (2012). NIH Image to ImageJ: 25 years of image analysis. Nature Methods **9,** 671-675.

Schnell, D.J., Kessler, F., and Blobel, G. (1994). Isolation of components of the chloroplast protein import machinery. Science **266,** 1007-1012.

Shanmugabalaji, V., Chahtane, H., Accossato, S., Rahire, M., Gouzerh, G., Lopez-Molina, L., and Kessler, F. (2018). Chloroplast biogenesis controlled by DELLA-TOC159 interaction in early plant development. Current Biology **28,** 2616-2623 e2615.

Sowden, R.G., Watson, S.J., and Jarvis, P. (2018). The role of chloroplasts in plant pathology. Essays in Biochemistry **62,** 21-39.

Sriramachandran, A.M., and Dohmen, R.J. (2014). SUMO-targeted ubiquitin ligases. Biochimica et Biophysica Acta **1843,** 75-85.

Tranel, P.J., Froehlich, J., Goyal, A., and Keegstra, K. (1995). A component of the chloroplastic protein import apparatus is targeted to the outer envelope membrane via a novel pathway. The EMBO Journal **14,** 2436-2446.

Tzfira, T., Tian, G.W., Lacroix, B., Vyas, S., Li, J., Leitner-Dagan, Y., Krichevsky, A., Taylor, T., Vainstein, A., and Citovsky, V. (2005). pSAT vectors: a modular series of plasmids for autofluorescent protein tagging and expression of multiple genes in plants. Plant Molecular Biology **57,** 503.

van den Burg, H.A., Kini, R.K., Schuurink, R.C., and Takken, F.L.W. (2010). *Arabidopsis* small ubiquitin-like modifier paralogs have distinct functions in development and defense. Plant Cell **22,** 1998-2016.

Watson, S.J., Sowden, R.G., and Jarvis, P. (2018). Abiotic stress-induced chloroplast proteome remodelling: a mechanistic overview. Journal of Experimental Botany **69,** 2773-2781.

Wu, F.H., Shen, S.C., Lee, L.Y., Lee, S.H., Chan, M.T., and Lin, C.S. (2009). Tape-Arabidopsis Sandwich - a simpler Arabidopsis protoplast isolation method. Plant Methods **5,** 16.

Zhao, Q., Xie, Y., Zheng, Y., Jiang, S., Liu, W., Mu, W., Liu, Z., Zhao, Y., Xue, Y., and Ren, J. (2014). GPS-SUMO: a tool for the prediction of sumoylation sites and SUMO-interaction motifs. Nucleic Acids Research **42,** W325-W330.

Acknowledgements

We are very grateful to Alistair Haslam for initiating the genetic experiments. We also thank Dr Errin Johnson and Raman Dhaliwal (Dunn School of Pathology, University of Oxford) for assistance with the electron microscopy, and Prof Jane Langdale for advice during the course of the work. We are grateful to Pedro Bota and Rita Ross for technical support. This work was supported by the Oxford Interdisciplinary Bioscience Doctoral Training Partnership (DTP), and by grants from the Biotechnology and Biological Sciences Research Council (BBSRC) (grant numbers BB/K018442/1, BB/N006372/1, BB/R016984/1 and BB/R009333/1) to RPJ.

Competing interests

The authors declare no competing interests.

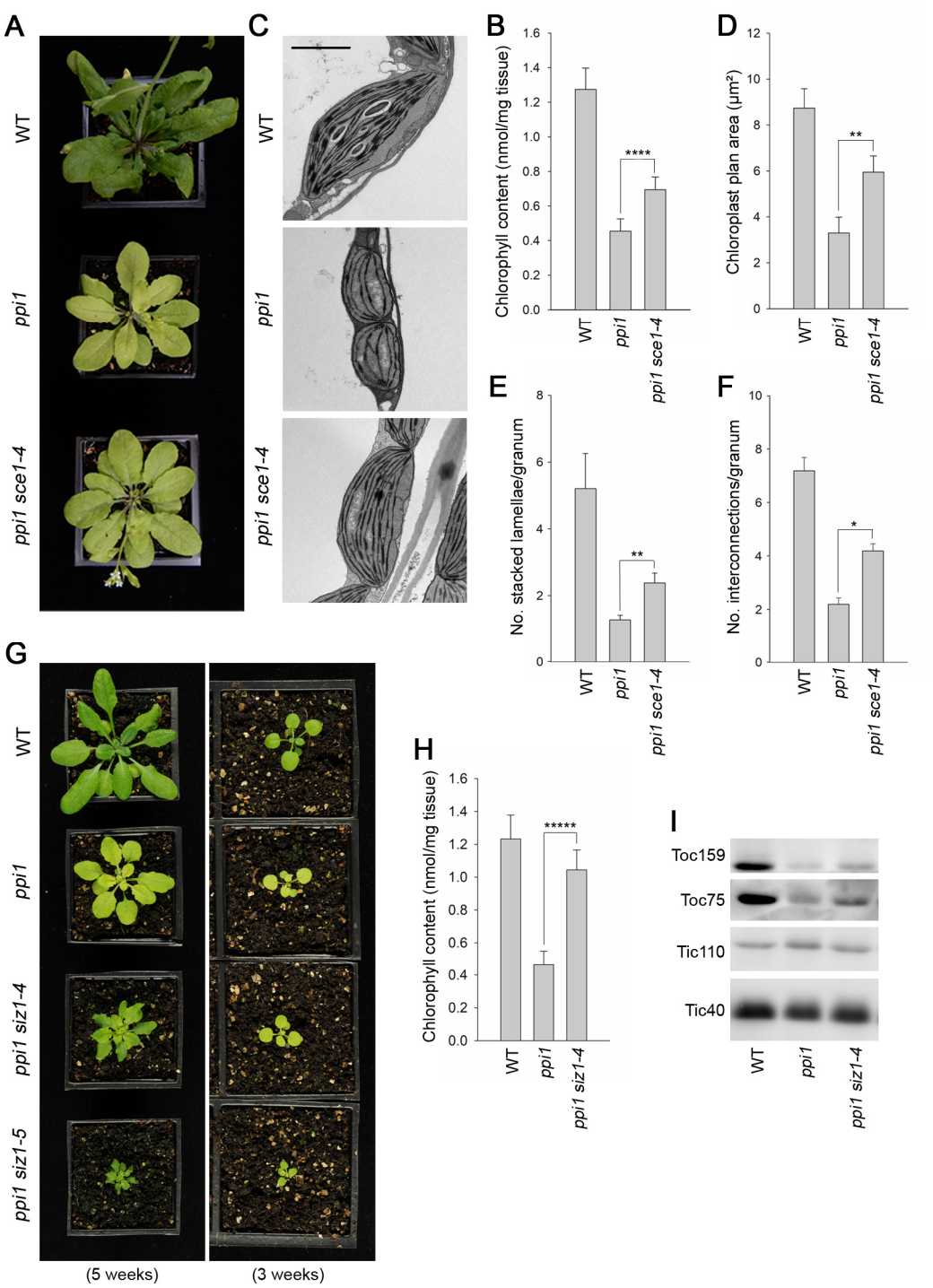

Figure 1

The E2 SUMO conjugating enzyme mutation, *sce1-4*, and the E3 SUMO ligase mutation, *siz1-4*, suppress the phenotype of plastid protein import mutant, *ppi1*.

(A) The *ppi1 sce1-4* double mutant appeared greener than *ppi1* after approximately five weeks of growth on soil.

(B) The *ppi1 sce1-4* double mutant showed enhanced accumulation of chlorophyll relative to *ppi1* after approximately five weeks of growth on soil. Measurements were taken from the plants shown in (A) on the day of photography, as well as additional similar plants. Error bars indicate standard

599 deviation from the mean (*n* = 7). There were significant differences between the *ppi1* and *ppi1 sce1-*
600 *4* plants (Two-tailed t-test, unpaired samples, T = 6.15, *p* = 0.000049).

601 (C) Transmission electron microscopy revealed improved chloroplast development in mature rosette
602 leaf mesophyll tissue of *ppi1 sce1-4* plants relative to *ppi1*. Plants that had been grown on soil for
603 approximately four weeks were analysed, and representative images are shown. Scale bar = 2 µm.

604 (D) Chloroplast plan area was elevated in *ppi1 sce1-4* relative to *ppi1*. The transmission electron
605 microscopy dataset was quantified. Error bars indicate standard deviation from the mean (*n* = 3
606 biological replicates). There were significant differences between the *ppi1* and *ppi1 sce1-4* plants
607 (Two-tailed t-test, unpaired samples, T = 4.65, *p* = 0.009674).

608 (E) Thylakoid membrane stacking was increased in *ppi1 sce1-4* relative to *ppi1*. The number of
609 stacked thylakoidal lamellae per granum was analysed. Error bars indicate standard error from the
610 mean (*n* = 3 biological replicates). There were significant differences between the *ppi1* and *ppi1*
611 *sce1-4* plants (Two-tailed t-test, unpaired samples, T = 5.53, *p* = 0.005221).

612 (F) Thylakoid membrane interconnections were increased in *ppi1 sce1-4* relative to *ppi1*. The
613 number of stromal thylakoidal lamellae emanating from each granum (granal interconnections) was
614 analysed. Error bars indicate standard error from the mean (*n* = 3 biological replicates). There were
615 significant differences between the *ppi1* and *ppi1 sce1-4* plants (Two-tailed t-test, unpaired samples,
616 T = 3.38, *p* = 0.0277).

617 (G) The *ppi1 siz1-4* and *ppi1 siz1-5* double mutants appeared greener than *ppi1* after different
618 periods of growth on soil. The plants were photographed after three weeks of growth (right panel)
619 and then again after five weeks of growth (left panel).

620 (H) The *ppi1 siz1-4* double mutant showed enhanced accumulation of chlorophyll relative to *ppi1*
621 after approximately five weeks of growth on soil. Measurements were taken from the plants shown
622 in (G) on the day of photography, as well as additional similar plants. Error bars indicate standard
623 deviation from the mean (*n* = 8). There were significant differences between the *ppi1* and *ppi1 siz1-4*
624 plants (Two-tailed t-test, unpaired samples, T = 11.01, *p* < 0.00001).

625 (I) TOC protein accumulation is improved in *ppi1 siz1-4* relative to *ppi1*. Analysis of the levels of
626 Toc75 and Toc159 in *ppi1 siz1-4* and relevant control plants was conducted by immunoblotting.
627 Protein samples were taken from the rosette tissue of plants that had been grown on soil for
628 approximately five weeks. Toc159 typically migrates as a complex series of bands owing to its
629 proteolytic sensitivity, and only the major band is shown. The TIC-associated proteins, Tic110 and
630 Tic40, were employed as controls.

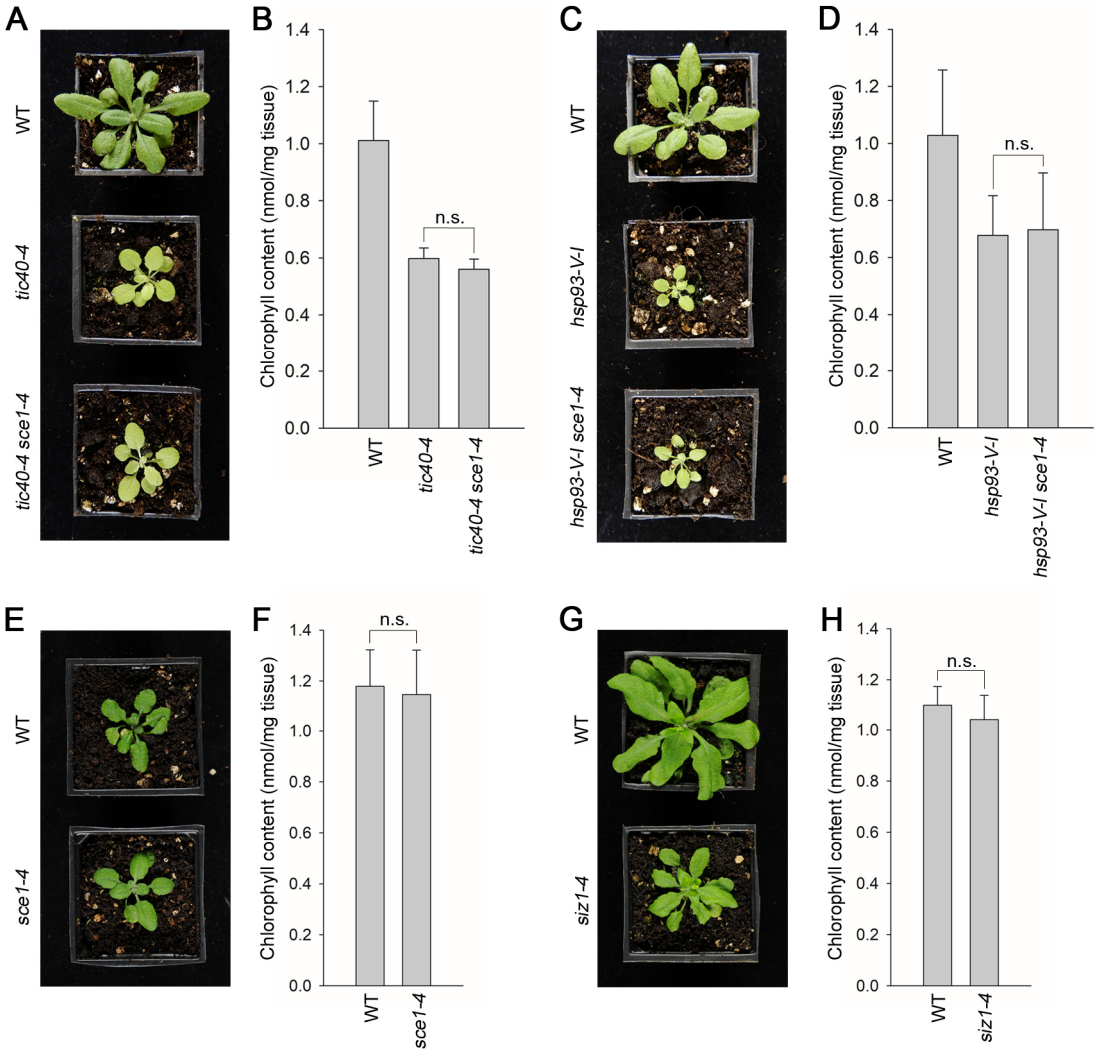

Figure 2

Genetic analysis reveals specificity of the suppression mediated by the *sce1-4* and *siz1-4* mutations.

(A) The *tic40-4 sce1-4* double mutant did not appear greener than *tic40-4* after approximately four weeks of growth on soil.

(B) The *tic40-4 sce1-4* double mutant did not show an enhanced accumulation of chlorophyll relative to *tic40-4* after approximately four weeks of growth on soil. Measurements were taken from the plants shown in (A) on the day of photography, as well as additional similar plants. Error bars indicate standard deviation from the mean (n = 3). There were no significant differences between the *tic40-4* and *tic40-4 sce1-4* plants (Two-tailed t-test, unpaired samples, T = 1.25, p = 0.280106).

(C) The *hsp93-V-I sce1-4* double mutant did not appear greener than *hsp93-V-I* after approximately four weeks of growth on soil.

(D) The *hsp93-V-I sce1-4* double mutant did not show an enhanced accumulation of chlorophyll relative to *hsp93-V-I* after approximately four weeks of growth on soil. Measurements were taken from the plants shown in (C) on the day of photography, as well as additional similar plants. Error bars indicate standard deviation from the mean (n = 5). There were no significant differences

between the *hsp93-V-I* and *hsp93-V-I sce1-4* plants (Two-tailed t-test, unpaired samples, T = 0.18, p = 0.860702).

(E) The *sce1-4* single mutant did not appear greener than wild-type plants after approximately four weeks of growth on soil.

(F) The *sce1-4* single mutant did not show an enhanced accumulation of chlorophyll relative to wild-type plants after approximately four weeks of growth on soil. Measurements were taken from the plants shown in (E) on the day of photography, as well as additional similar plants. Error bars indicate standard deviation from the mean (n = 7). There were no significant differences between the *sce1-4* and wild type plants (Two-tailed t-test, unpaired samples, T = 0.38, p = 0.708484).

(G) The *siz1-4* single mutant did not appear greener than wild-type plants after approximately five weeks of growth on soil.

(H) The *siz1-4* single mutant did not show an enhanced accumulation of chlorophyll relative to wild-type plants after approximately five weeks of growth on soil. Measurements were taken from the plants shown in (G) on the day of photography, as well as from additional similar plants. Error bars indicate standard deviation from the mean (n = 4-5). There were no significant differences between the *siz1-4* and wild type plants (T = 0.96, p = 0.370055).

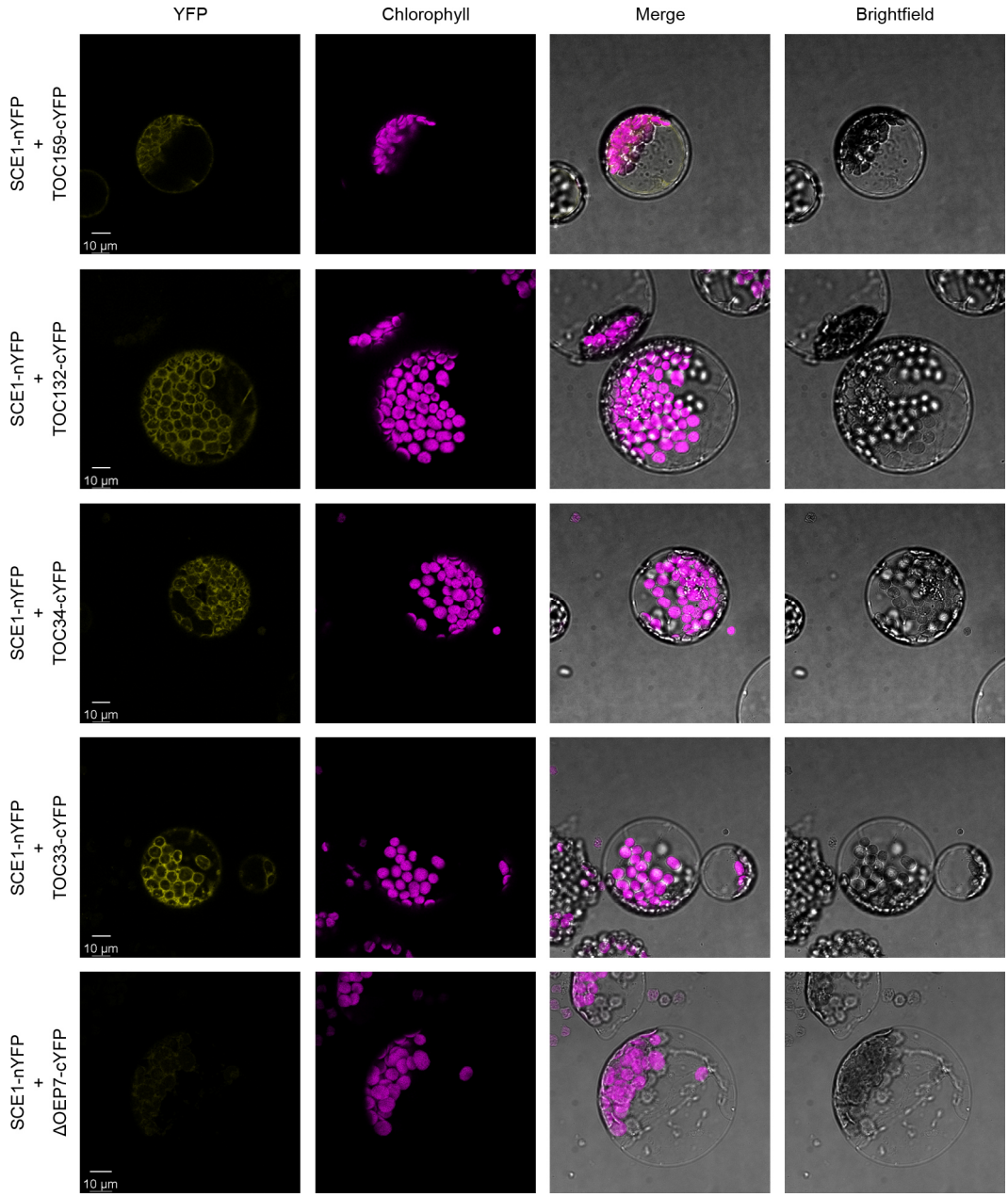

665

666 **Figure 3**

667 **SCE1 physically interacts with TOC proteins *in vivo.***

668 Bimolecular fluorescence complementation (BiFC) analysis of SCE1 protein-protein interactions was
669 performed by imaging *Arabidopsis* protoplasts co-expressing proteins fused to complementary N-
670 terminal (nYFP) and C-terminal (cYFP) fragments of the YFP protein, as indicated. Chlorophyll
671 autofluorescence images were employed to orientate the YFP signals in relation to the chloroplasts.
672 In this analysis, SCE1 physically associated with TOC proteins. The images shown are representative
673 confocal micrographs indicating associations between SCE1 and Toc159, Toc132, Toc34 and Toc33.
674 In contrast, SCE1 did not physically associate with ΔOEP7-cYFP (comprising the transmembrane
675 domain of OEP7, which is sufficient to direct targeting to the chloroplast outer envelope, fused to
676 the cYFP fragment), which served as a negative control. Scale bars = 10 µm.

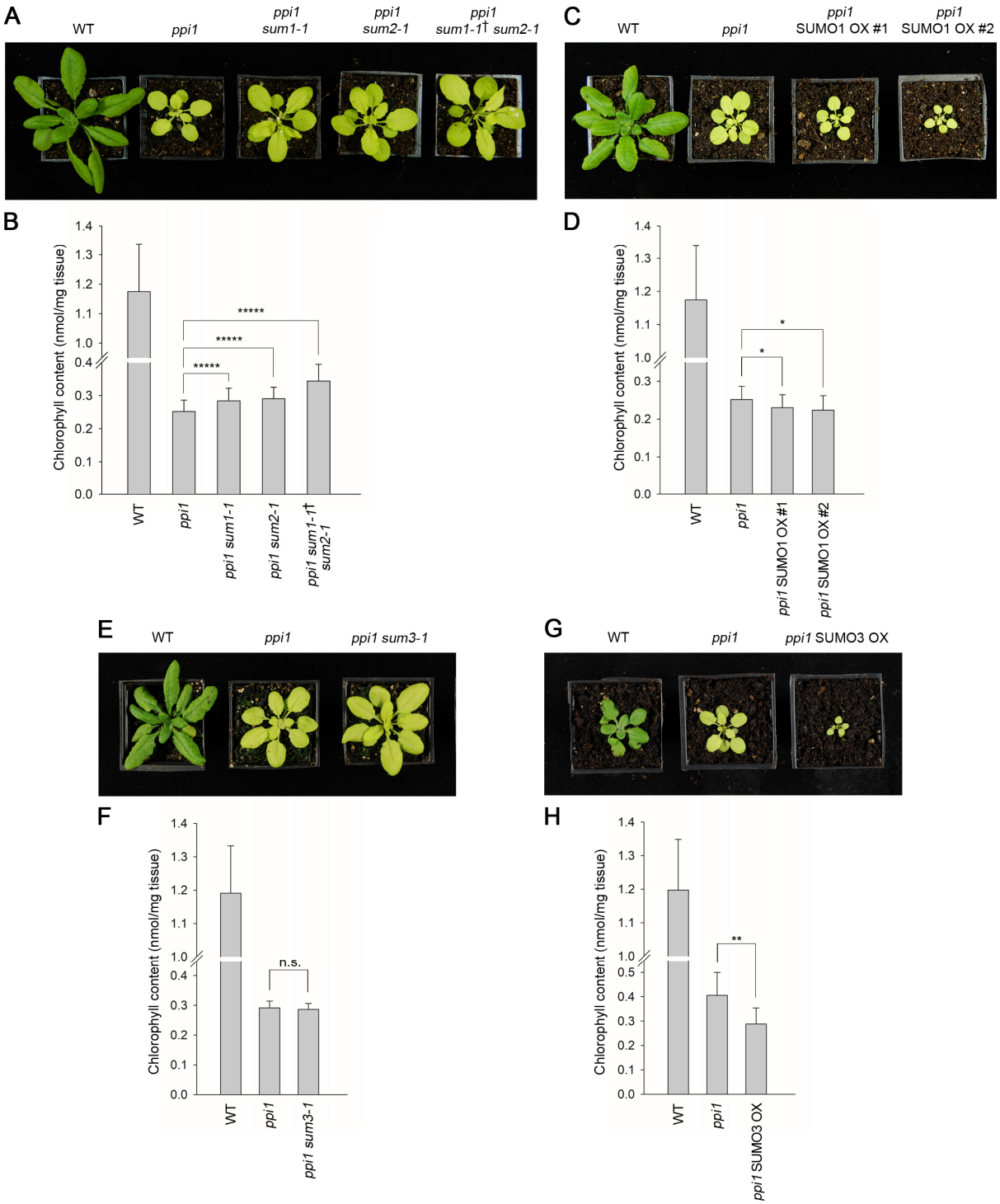

Figure 4

Genetic interactions between *ppi1* and the genes encoding three SUMO isoforms.

(A) The *ppi1 sum1-1, ppi1 sum2-1,* and *ppi1 sum1-1† sum2-1* double and triple mutants appeared greener than *ppi1* after approximately four weeks of growth on soil. The dagger symbol indicates that the triple mutant was heterozygous with respect to the *sum1-1* mutation.

(B) The *ppi1 sum1-1, ppi1 sum2-1,* and *ppi1 sum1-1† sum2-1* double and triple mutants showed enhanced accumulation of chlorophyll relative to *ppi1* after approximately four weeks of growth on soil. Measurements were taken from the plants shown in (A) on the day of photography, as well as

686 additional similar plants. Error bars indicate standard deviation from the mean (*n* = 20-71). There
687 were significant differences between the samples, as measured via a one-way ANOVA (F = 26.21, *p* =
688 6.65×10^{-14}). A post-hoc Tukey HSD test indicated that there was a significant difference between
689 the *ppi1* and *ppi1 sum1-1* samples ($p < 0.00001$). There were also significant differences between the
690 *ppi1* and *ppi1 sum2-1* samples ($p < 0.00001$), and between the *ppi1* and *ppi1 sum1-1* sum2-1*
691 samples ($p < 0.00001$).

692 (C) The *ppi1* SUMO1 overexpression (OX) lines appeared smaller and paler than *ppi1* after
693 approximately four weeks of growth on soil.

694 (D) The *ppi1* SUMO1 OX lines showed reduced accumulation of chlorophyll relative to *ppi1* after
695 approximately four weeks of growth on soil. Measurements were taken from the plants shown in (C)
696 on the day of photography, as well as additional similar plants. Error bars indicate standard deviation
697 from the mean (*n* = 24-37). There were significant differences between the *ppi1* and *ppi1* SUMO1 OX
698 #1 plants (Two-tailed t-test, unpaired samples, T = 2.27, *p* = 0.026832), and between the *ppi1* and
699 *ppi1* SUMO1 OX #2 plants (Two-tailed t-test, unpaired samples, T = 2.49, *p* = 0.01634).

700 (E) The *ppi1 sum3-1* double mutant did not appear greener than *ppi1* after approximately four
701 weeks of growth on soil.

702 (F) The *ppi1 sum3-1* double mutant did not show an enhanced accumulation of chlorophyll relative
703 to *ppi1* after approximately four weeks of growth on soil. Measurements were taken from the plants
704 shown in (E) on the day of photography, as well as additional similar plants. Error bars indicate
705 standard deviation from the mean (*n* = 10). There were no significant differences between the *ppi1*
706 and *ppi1 sum3-1* plants (Two-tailed t-test, unpaired samples, T = 0.54, *p* = 0.59407).

707 (G) The *ppi1* SUMO3 overexpression line appeared smaller and paler than *ppi1* after approximately
708 three weeks of growth on soil.

709 (H) The *ppi1* SUMO3 overexpression line showed reduced accumulation of chlorophyll relative to
710 *ppi1* after approximately three weeks of growth on soil. Measurements were taken from the plants
711 shown in (G) on the day of photography, as well as additional similar plants. Error bars indicate
712 standard deviation from the mean (*n* = 8-10). There were significant differences between the *ppi1*
713 SUMO3 OX plants and *ppi1* (Two-tailed t-test, unpaired samples, T = 2.99, *p* = 0.008688).

714

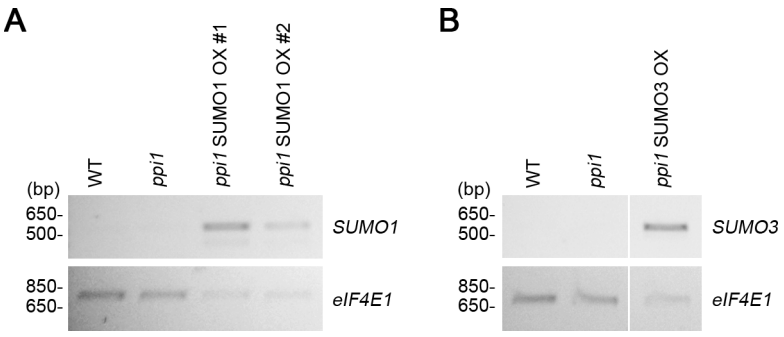

Figure 4 supplement

Analysis of the expression of the 35S:*SUMO1* and 35S:*SUMO3* transgenes in the selected transformants by RT-PCR.

Total RNA was extracted from the rosette tissue of plants that had been grown on soil for approximately four weeks. The expression of *SUMO1* (A) or *SUMO3* (B), and of the control gene, *eIF4E1*, was analysed by semi-quantitative RT-PCR. A limited number of amplification cycles (*n* = 26) was employed to prevent saturation. Migration positions of standards are displayed to the left of the gel images.

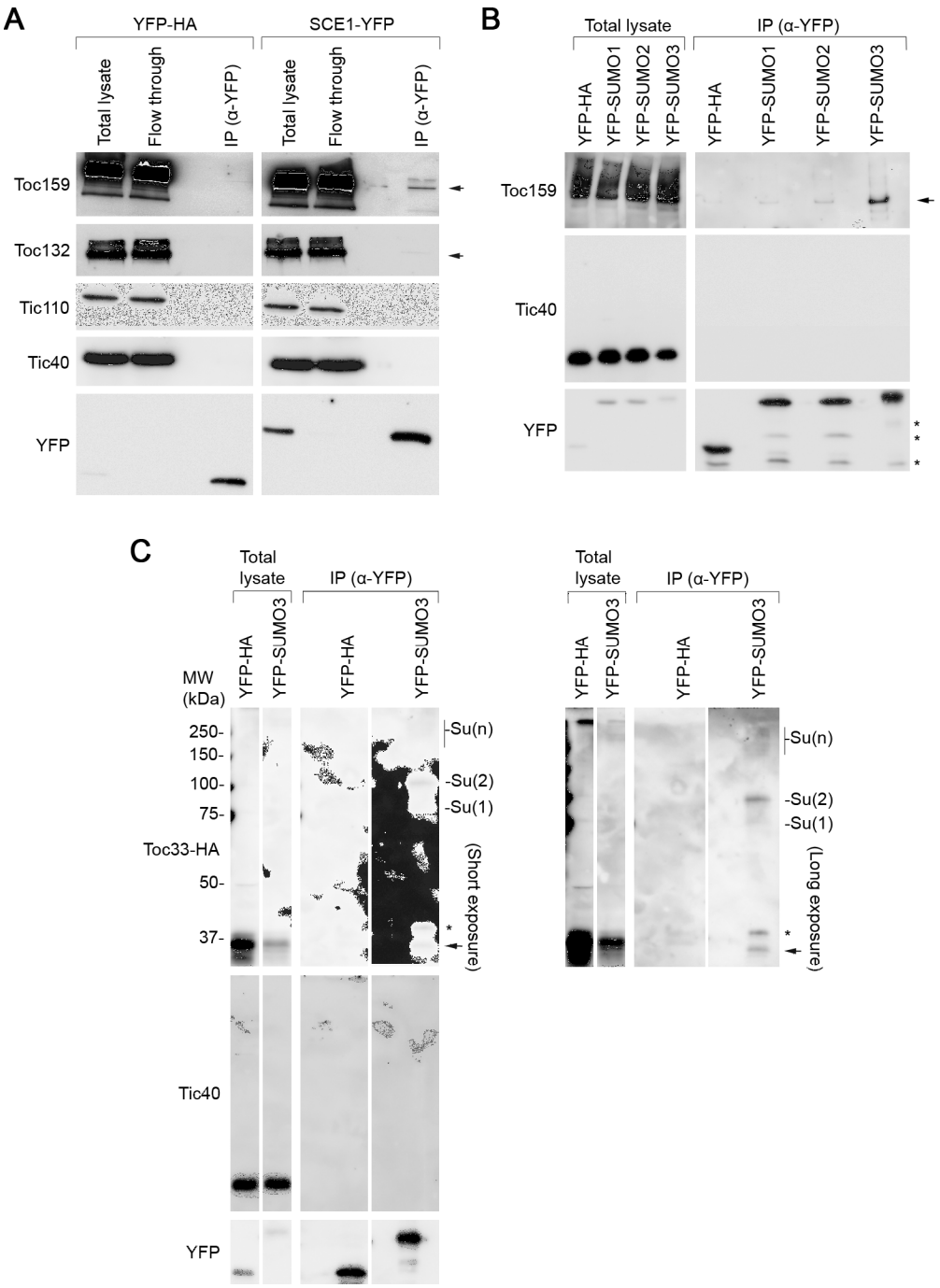

Figure 5

Immunoprecipitation analysis reveals that TOC proteins are SUMO targets.

(A) SCE1 physically associated with native TOC proteins. *Arabidopsis* protoplasts expressing YFP-HA (left panel) or SCE1-YFP (right panel) were solubilised and subjected to immunoprecipitation (IP) analysis. The YFP-HA construct served as a negative control. In both cases, three samples were analysed: The 'Total lysate' sample (total protein extract from solubilised protoplasts); the 'Flow through' sample (the total protein sample after incubation with anti-YFP beads); and the 'IP' sample (the eluted fraction of the total protein sample that bound to the anti-YFP beads). The samples were analysed by immunoblotting, revealing that SCE1-YFP, but not the YFP-HA control, was associated with native Toc159 and Toc132 (indicated by the two arrows). Neither SCE1-YFP nor YFP-HA was associated with native Tic110 or Tic40, which were employed as negative control proteins.

(B) All three SUMO isoforms physically associated with native Toc159. Protoplasts expressing YFP-HA, YFP-SUMO1, YFP-SUMO2 or YFP-SUMO3 were solubilised and subjected to IP analysis as in (A). In all four cases, two samples (the 'Total lysate' and the 'IP' samples) were analysed by immunoblotting. Toc159 was resolved on an 8% acrylamide gel for four hours to maximise the resolution of high molecular weight bands. All three YFP-SUMO proteins were found to associate with native Toc159 (indicated by the arrow); however, YFP-SUMO3 immunoprecipitated Toc159 with the greatest efficiency. Analysis of a long exposure of the YFP blot revealed the presence of high molecular weight bands, for all three YFP-SUMO fusion proteins, consistent with the formation of SUMO conjugates. None of the four YFP fusion proteins associated with native Tic40, which served as a negative control protein. The asterisks indicate non-specific bands.

(C) YFP-SUMO3 physically associated with Toc33-HA and related high molecular weight species. Protoplasts co-expressing YFP-SUMO3 or YFP-HA together with Toc33-HA were solubilised and subjected to IP analysis as in (A). In both cases, two samples (the 'Total lysate' and 'IP' samples) were analysed by immunoblotting. The results showed that YFP-SUMO3, but not YFP-HA, was associated with Toc33-HA (indicated by the arrow). Bands corresponding to the molecular weight of Toc33-HA bearing one, two or several YFP-SUMO3 motifs were also detected on the membrane (indicated as Su(1), Su(2), and Su(n)). The predicted molecular weight of YFP-SUMO3 is approximately 38.9 kDa. Neither YFP-SUMO3 nor YFP-HA was associated with Tic40, which served as a negative control protein. The asterisk indicates a nonspecific band.

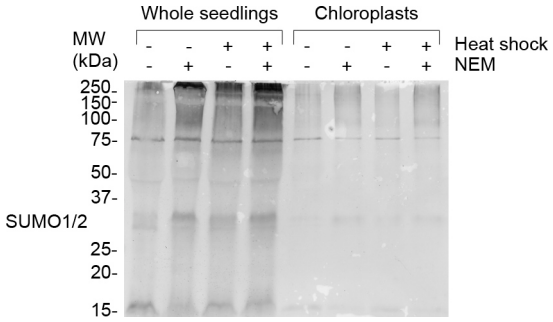

Figure 5 supplement 1

Chloroplast resident proteins are SUMOylated.

Anti-SUMO1 immunoblot analysis of protein samples taken from whole seedlings (left hand side) and isolated chloroplasts (right hand side). Where indicated, the samples were exposed to heat shock (42°C for 30 seconds) and/or incubated with 10 mM NEM to aid the detection of SUMOylated proteins. The anti-SUMO1 antibody used is known to show significant cross-reactivity with SUMO2 (Kurepa et al., 2003).

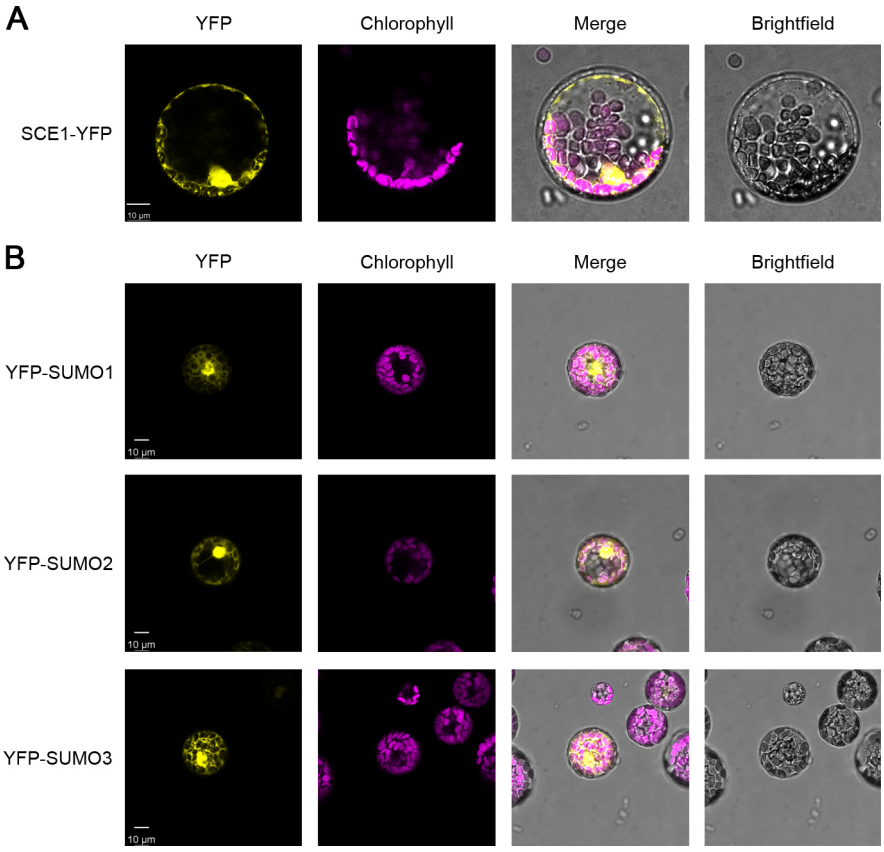

Figure 5 supplement 2

Analysis of the expression of the YFP-tagged constructs used in the immunoprecipitation experiments by confocal microscopy.

The expression of the SCE1-YFP construct (A), and of the three YFP-SUMO constructs (B), was analysed and confirmed by imaging transfected *Arabidopsis* protoplasts. Chlorophyll autofluorescence images were employed to orientate the YFP signals in relation to the chloroplasts. Representative confocal micrographs show a typical protoplast in each case. Scale bars = 10 µm.

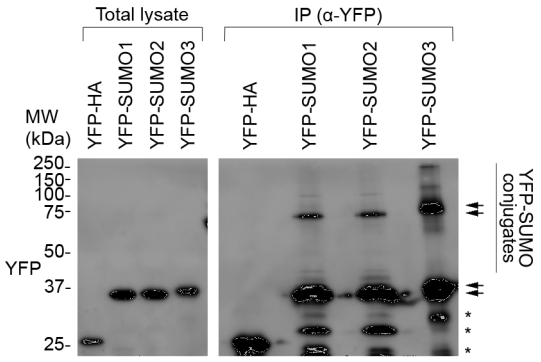

774

775 **Figure 5 supplement 3**

776 **All three YFP-SUMO probes are conjugation-competent.**

777 The membrane shown is the same as the one presented in Figure 5B (YFP panel). In this case, the
778 membrane was visualised using a long exposure to aid the detection of weakly abundant protein
779 bands. As well as the YFP-SUMO monomers, additional high molecular bands and smears were seen
780 in the IP samples, indicating the capture of large numbers of SUMOylated proteins. This shows that
781 all three YFP-SUMO probes could be successfully conjugated, as expected (Ayaydin and Dasso,
782 2004). The positions of the YFP-SUMO monomers (lower pair of arrows), and of the various SUMO
783 adducts (vertical bar) potentially including di-SUMO (upper pair of arrows), are indicated. Note that
784 YFP-SUMO3 migrated more slowly than the other two fusions, as expected. The asterisks indicate
785 non-specific bands.

786

Table 1

Bioinformatic analysis predicts that the core TOC proteins in *Arabidopsis* contain SUMOylation sites and SUMO interaction motifs.

The GPS-SUMO algorithm was applied to the amino acid sequences of Toc159, Toc132, Toc120, Toc90, Toc75, Toc33 and Toc34 using the 'high stringency' setting, and the results generated are shown in columns 2, 3 and 4. 'Consensus' sites fall within canonical SUMO site motifs: ψ-K-X-E (where ψ indicates a hydrophobic amino acid, and X indicates any amino acid residue). 'Non-consensus' sites do not fall within canonical SUMO site motifs; analysis shows that ~40% of SUMOylation may occur at non-consensus sites (Zhao et al., 2014). 'SUMO Interaction' sites are predicted to mediate the non-covalent interaction between proteins and SUMO peptides. The JASSA algorithm was also applied to the amino acid sequences using the 'high cut-off' setting (see column 5). aa denotes amino acids.

Protein name	Position (aa)	*p*-value	Type	Also predicted by JASSA (high stringency)?
atToc159	95	0.021	Consensus	No
(At4g02510)	106	0.034	Consensus	Yes
1503 aa	126	0.032	Consensus	Yes
	144	0.02	Consensus	Yes
	151	0.02	Consensus	No
	246-250	0.005	SUMO Interaction	Yes
	408-412	0.009	SUMO Interaction	Yes
	486-490	0.009	SUMO Interaction	Yes
	498	0.022	Consensus	No
	502	0.049	Non-consensus	No
	539	0.026	Consensus	No
	1300	0.049	Non-consensus	No
	1370	0.01	Consensus	Yes
atToc132	30	0.006	Consensus	Yes
(At2g16640)	66	0.036	Consensus	Yes
1206 aa	352	0.002	Consensus	No
	895	0.005	Consensus	No
	1077	0.014	Consensus	No
atToc120	52	0.008	Consensus	No
(At3g16620)	57	0.031	Consensus	No
1084 aa	209	0.05	Non-consensus	No
	777	0.006	Consensus	No
	959	0.013	Consensus	No
atToc90	191	0.027	Consensus	Yes
(At5g20300)	481	0.017	Consensus	No
793 aa	711	0.02	Consensus	No
	786	0.042	Non-consensus	Yes

atToc75 (At3g46740) 818 aa	434 513	0.049 0.029	Non-consensus Consensus	No No
atToc33 (At1g02280) 297 aa	291	0.044	Non-consensus	No
atToc34 (At5g05000) 313 aa	290 298	0.026 0.043	Consensus Non-consensus	No Yes

800

801

802 **Table 2**

803 **Primers used during the course of this study.**

804 (A) Primers used in restriction cloning procedures.

Primer name	Sequence*	Used to generate…
SCE1 F (HindIII)	AAAAGCTTATGGCTAGTGGAATCGCTC	pSAT4(A)-nEYFP-N1 SCE1
SCE1 R (EcoRI)	AAGAATTCGACAAGAGCAGGATACTGCTTG	pSAT4(A)-nEYFP-N1 SCE1
Toc159-5 F (EcoRI)	AAGAATTCAATGGACTCAAAGTCGGTT	pSAT4-cEYFP-C1-B Toc159
Toc159-3 R (SalI)	AAGTCGACTTAGTACATGCTGTACTT	pSAT4-cEYFP-C1-B Toc159
Toc132-5 F (XhoI)	AACTCGAGCTATG GGAGATGGGACTGAG	pSAT4-cEYFP-C1-B Toc132
Toc132-3 R (SmaI)	AACCCGGGTCATTGTCCATATTGCGT	pSAT4-cEYFP-C1-B Toc132
Toc33-5 F (HindIII)	AGAAGCTTCGATGGGGTCTCTCGTTCGT	pSAT4-cEYFP-C1-B Toc33
Toc33-3 R (XbaI)	AATCTAGATTAAAGTGGCTTTCCACT	pSAT4-cEYFP-C1-B Toc33
Toc34-5 F (HindIII)	AGAAGCTTCGATGGCAGCTTTGCAAACG	pSAT4-cEYFP-C1-B Toc34
Toc34-3 R (XbaI)	AATCTAGATCAAGACCTTCGACTTGC	pSAT4-cEYFP-C1-B Toc34
OEP7 F (XhoI)	CTCGAGATGGGAAAAACTTCGGGA	pSAT4(A)-cEYFP-N1 ΔOEP7
OEP7-35 R (KpnI)	GGTACCGGAATTTATCGAGGAAAGG	pSAT4(A)-cEYFP-N1 ΔOEP7
SFR2 F (KpnI)	GGTACCAACTAGAAAGATCCGGTG	pSAT4(A)-cEYFP-N1 SFR2
SFR2-ns R (XmaI)	CCCGGGGTCAAAGGGTGAGGCTAA	pSAT4(A)-cEYFP-N1 SFR2

805

806 (B) Primers used in Gateway cloning procedures.

Primer name	Sequence*	Used to generate…
SCE1 Gateway F	GGGGACAAGTTTGTACAAAAAAGCAGGCTCCATGGCTAGTGGAATCGCTC	p2GWY7 SCE1
SCE1 Gateway R	GGGGACCACTTTGTACAAGAAAGCTGGGTTGACAAGAGCAGGATACTGC	p2GWY7 SCE1
SUMO1 Gateway F	GGGGACAAGTTTGTACAAAAAAGCAGGCTCCTCTGCAAACCAGGAGGAAGACAAG	p2YGW7 SUMO1
SUMO1 Gateway R	GGGGACCACTTTGTACAAGAAAGCTGGGTTTCAGGCCGTAGCACCACC	p2YGWY SUMO1
SUMO2 Gateway F	GGGGACAAGTTTGTACAAAAAAGCAGGCTCCTCTGCTACTCCGGAAGAAGAC	p2YGW7 SUMO2
SUMO2 Gateway R	GGGGACCACTTTGTACAAGAAAGCTGGGTTCTAAAAGCAGAAGAGCTTCAGGCC	p2YGW7 SUMO2
SUMO3 Gateway F	GGGGACAAGTTTGTACAAAAAAGCAGGCTCCTCTAACCCTCAAGATGACAAGCCC	p2YGW7 SUMO3
SUMO3 Gateway R	GGGGACCACTTTGTACAAGAAAGCTGGGTTTTAAAGCCCATTATGATCGAAAAGC	p2YGW7 SUMO3

807

808 (C) Primers used in RT-PCR experiments.

Primer name	Sequence	Used to amplify…
SUMO1 F(2)	AAAAAGCAGGCTCCACAAAAGCCACGGCCAATTAG	*SUMO1*
SUMO1 R(2)	AGAAAGCTGGGTTCCATTCATATCACACACAAGCCC	*SUMO1*
SUMO3 F	ACAGACTGGAGTTTTTGTTTC	*SUMO3*
SUMO3 R	CTCATGAGTCATTTACACACACG	*SUMO3*
eIF4E1 F	AAGATTTGAGAGGTTTCAAGCGGTGTAAG	*eIF4E1*
eIF4E1 R	AAACAATGGCGGTAGAAGACACTC	*eIF4E1*

809

810 (D) Primers used to genotype mutants.

Primer name	Sequence	Used to genotype…
SUMO1 F(2)	AAAAAGCAGGCTCCACAAAAGCCACGGCCAATTAG	*sum1-1*

SUMO1 R(2)	AGAAAGCTGGGTTCCATTCATATCACACACAAGCCC	*sum1-1*
SUMO2 F	CGTTGTTGGTACTTGGTTGG	*sum2-1*
SUMO2 R	CAAAACTCTAAACTGGTCGG	*sum2-1*
SUMO3 F	ACAGACTGGAGTTTTTGTTTC	*sum3-1*
SUMO3 R	CTCATGAGTCATTTACACACACG	*sum3-1*
SCE1 F	CGCCGCGAAATCTGGACC	*sce1-4*
SCE1 R	TTCCTCTCTTCAGCTAAACG	*sce1-4*
SIZ1 F(2)	GCAAACAGGGAAAGAAGCAGG	*siz1-4*
SIZ1 R(2)	CATTGAGTCTGTTTCTAGCG	*siz1-4*
LBb1	GCGTGGACCGCTTGCTGCAACT	SALK lines (left border)
LB1	GCCTTTTCAGAAATGGATAAATAGCCTTGCTTCC	SAIL lines (left border)

811

812 * Restriction sequences are underlined.